

# Analytical model for heterogeneous crystallization kinetics of spherical glass particles

V. Lopez-Richard,<sup>1</sup> Eduardo Bellini Ferreira,<sup>2,\*</sup> Edgar Dutra Zanotto,<sup>3</sup> and G. E. Marques<sup>1</sup>

<sup>1</sup>*Departamento de Física, Universidade Federal de São Carlos, 13.565-905, São Carlos, São Paulo, Brazil*

<sup>2</sup>*Vitrovita Instituto de Inovação em Vitrocerâmicos, 13560-460, São Carlos, São Paulo, Brazil*

<sup>3</sup>*Vitreous Materials Laboratory, Department of Materials Engineering, Universidade Federal de São Carlos, 13.565-905, São Carlos, São Paulo, Brazil*

(Dated: September 20, 2008)

An analytical model developed to describe the crystallization kinetics of spherical glass particles has been derived in this work. A continuous phase transition from 3D-like to 1D-like crystal growth has been considered and a procedure for the quantitative evaluation of the critical time for this 3D-1D transition is proposed. This model also allows straightforward determination of the density of surface nucleation sites on glass powders using differential scanning calorimetry data obtained under different thermal conditions.

PACS numbers: 61.43.Fs, 64.70.kj, 81.05.Kf, 81.70.Pg,

Important surface crystallization related phenomena, such as the vitrification ability of any supercooled liquid and the kinetic competition between viscous flow sintering and surface crystallization of glass powders<sup>1,2</sup>, are commonly calculated by using an estimated number of heterogeneous nucleation sites per unit surface,  $N_s = n/(N \cdot S_g)$ . In this approach, it is assumed that a number  $N$  of equal-size glass particles having surface area,  $S_g$ , can be formed with a total number of crystallization sites,  $n$ . However, there is no unambiguous and simple method to determine  $N_s$  from direct measurements<sup>3</sup>. The value of  $N_s$  along with the average particle radius,  $R$ , size distribution and the linear growth rate,  $u$ , play a crucial role on the particle crystallization kinetics<sup>4-7</sup>. In this article, we derived a simplified model to account for the nucleation and growth of crystals (of simple geometry) on spherical glass particles. This modeling is based on a proper use of universal parameters and enables a simulation of the whole process and all its stages, which vary from three-dimensional (3D) growth from a glass particle surface to one-dimensional (1D) growth toward its interior.

In Fig. 1 we show an example of sequential crystal growth steps during the sintering of diopside ( $CaO.MgO.2SiO_2$ ) glass powders. The micrographs correspond to annealing steps performed at 825 °C for 2h (a), 4h (b), and 8h (c). After 2h of thermal treatment, crystal formation can be detected around the vitreous grains, shown by light dots in Fig. 1 (a). After impingement of the crystals on the surface of the glass grains [Fig. 1 (b)], 1D growth prevails, ( $t > 4h$ ). This process finally leads to the complete transformation of the former vitreous phase into crystals that grow from the surface towards the grain interior [Fig. 1 (c)]. These samples were further characterized by differential scanning calorimetry (DSC), as shown by the corresponding graphics on the right hand side of Fig. 1.

In order to characterize the crystallization of glass particles as a function of annealing time,  $t$ , we assume heterogeneous nucleation of cylindrical crystals growing at a linear rate,  $u$ , from a fixed number of sites per unit area,

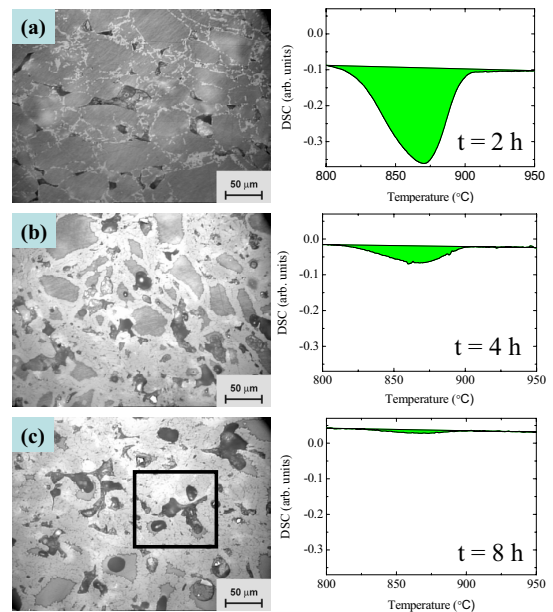


FIG. 1: Left: Micrographs of polished sections of diopside glass particles sintered at 825 C for: (a) 2 h, (b) 4 h and (c) 8 h. Color scale: light-gray phase = crystals; medium-dark grey phase = glass; from dark gray to black and eventually white in the center due to reflecting light = pores. Right: the corresponding DSC spectra of samples subjected to the different annealing steps at 825 °C before the DSC runs.

$N_s$ . Such growth takes place from the surface of the glass grains, with the circular base growing at the particles surface, and the cylindrical axis growing perpendicular to the surface toward their interior. According to the Johnson-Mehl-Avrami-Kolmogorov (JMAK) theory<sup>8-10</sup>, the crystalline volume fraction of a packing of spherical glass particles of radius  $R$  can be given by<sup>3</sup>

$$\alpha_v(t, N_s) = 1 - \exp(-3\alpha_s(t, N_s)u \cdot t/R). \quad (1)$$

Let us consider a sample with total volume,  $V_T$ , where the parameter  $\alpha_v = V_c/V_T$  characterizes the fraction of

$V_T$  that has been crystallized,  $V_c$  is the total volume occupied by crystals,  $\alpha_s = S_c/S_g$  is the fraction of crystallized surface, defined by the ratio between the crystallized area,  $S_c$  and the glass particle surface,  $S_g$ . The surface crystals reduce the effective surface of the glass particles available for further crystallization. Again, according to the JMAK theory<sup>11</sup>, the fraction of crystalline surface characterizing this 2D-growth is given by

$$\alpha_s(t, N_s) = 1 - \exp(-\pi N_s u^2 t^2). \quad (2)$$

Let us now introduce some universal (reduced) parameters  $\tau \equiv u \cdot t/R$  and  $\nu_s \equiv 4\pi R^2 N_s$ . One should observe that  $\tau$  is proportional to the growth rate of the linear length of the cylindrical crystalline region and to the radius of the spherical glass particles,  $R$ , (thus,  $\tau \in [0, 1]$ ) and  $\nu_s$  is the absolute number of nucleation sites on the surface of a spherical glass particle. With these new parameters, Eqs. (1) and (2) can be rewritten as

$$\alpha_s(\tau, \nu_s) = 1 - \exp(-\nu_s \cdot \tau^2/4), \quad (3)$$

and

$$\alpha_v(\tau, \nu_s) = 1 - \exp(-3\alpha_s(\tau, \nu_s) \cdot \tau), \quad (4)$$

respectively. Thus, the whole kinetic process depends only on dimensionless parameters: the effective time,  $\tau$ , and  $\nu_s$ . The surface and volume time-evolution growth, as expressed in Eqs. (3) and (4), are universal because they do not explicitly depend on any specific glass composition or temperature. The above equations can be directly linked to the DSC measurements.

It has been experimentally confirmed that the area under the DSC crystallization peak of partially crystallized samples,  $A(\tau, \nu_s)$  (the filled contours in the right panels of Fig. 1) is proportional to the remaining glassy volume,  $\alpha_g(\tau, \nu_s) V_T = (1 - \alpha_v(\tau, \nu_s)) V_T$ , where  $\alpha_g(\tau, \nu_s)$  is the glass volume fraction in these samples<sup>12,13</sup>. Thus,  $A(\tau, \nu_s) \propto V_T [1 - \alpha_v(\tau, \nu_s)]$ .

The total volume can be expressed by the ratio between the sample mass,  $m$ , and the density of the solid material,  $\rho_T = \rho_g + \alpha_v(\tau, \nu_s) [\rho_g - \rho_c]$ , which is defined by the crystallized volume fraction and the mass densities of the crystal and glass phases,  $\rho_c$  and  $\rho_g$ , respectively, as  $V_T(\tau) = m / (\rho_g + \alpha_v(\tau, \nu_s) [\rho_g - \rho_c])$ . Now, considering equal-mass samples, it is possible to obtain the ratio between the area under a DSC crystallization peak, at any given time of the crystallization process,  $A(\tau, \nu_s)$ , and the area at  $t = 0$ ,  $A(0, \nu_s)$  as

$$\frac{A(\tau, \nu_s)}{A(0, \nu_s)} = \left( 1 + \frac{\alpha_v(\tau, \nu_s)}{[1 - \alpha_v(\tau, \nu_s)]} \frac{\rho_c}{\rho_g} \right)^{-1}. \quad (5)$$

Hence, this equation yields a universal pattern, establishing a direct relationship between the dimensionless parameters  $\tau$  and  $\nu_s$ , and the ratio between mass densities,  $\rho_c/\rho_g$ .

In Fig. 2 (a), the function  $A(\tau, \nu_s)/A(0, \nu_s)$  is displayed for different values of  $\nu_s$ , for the ratio  $\rho_c/\rho_g = 1$ .

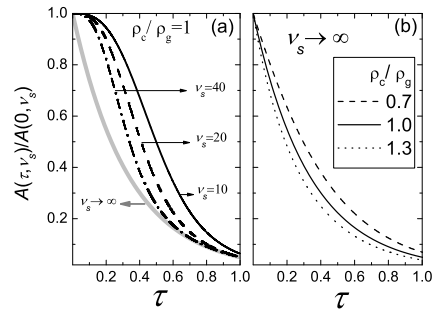


FIG. 2: (a) Plot of  $A(\tau, \nu_s)/A(0, \nu_s)$  for  $\rho_c/\rho_g = 1$  and different values of the universal parameter  $\nu_s$ . The limiting case, corresponding to large values of  $\nu_s$  is indicated by the thick grey solid curve. (b) Plot of  $A(\tau, \nu_s)/A(0, \nu_s)$ , in the limiting case  $\nu_s \rightarrow \infty$ , for a few values of the ratio  $\rho_c/\rho_g$ .

Under this condition, for large values for  $N_s$  and  $\nu_s$ , the crystallization process can be characterized as 1D. Such crystal growth conditions can be often observed, as shown for example in Figs. 1 (b) and (c) for diopside glass samples annealed at 825 °C for over 4 h, where the surface of the original glass particles is totally crystallized. In the limiting case of large  $N_s$  or, according to Eq. 4, for  $\nu_s \rightarrow \infty$ , the value of the crystalline volume fraction becomes  $\alpha_v(\tau, \infty) = 1 - \exp(-3 \cdot \tau)$ . The corresponding values of  $A(\tau, \infty)/A(0, \infty)$ , for  $\rho_c/\rho_g = 1$ , have been indicated in Fig. 2 (a) by a thick solid grey curve. They determine the lowest limit of  $A(\tau, \nu_s)/A(0, \nu_s)$ , for any possible combination of parameters. The dependence on the density ratio  $\rho_c/\rho_g$  can be seen in Fig. 2 (b), by setting  $\nu_s \rightarrow \infty$  within the interval  $\rho_c/\rho_g \in [0.7, 1.3]$ . Thus, the volume fraction  $\alpha_v(\tau, \nu_s)$  can be expressed as a function of the area and mass density ratios,  $A(\tau, \nu_s)/A(0, \nu_s)$ , and  $\rho_c/\rho_g$ , after using Eq. (5), in the form

$$\alpha_v(\tau, \nu_s) = \left( \frac{\rho_c}{\rho_g} \frac{A(\tau, \nu_s)/A(0, \nu_s)}{[1 - A(\tau, \nu_s)/A(0, \nu_s)]} + 1 \right)^{-1}. \quad (6)$$

One should note that simple DSC measurements performed with two samples with the same mass, a partially crystallized and a glassy one, provide the crystallized volume fraction  $\alpha_v(\tau, \nu_s)$  of materials with known density ratio  $\rho_c/\rho_g$ . By knowing  $u$  and  $R$ , one obtains  $\alpha_s(\tau, \nu_s)$  from Eq. (6) and together with Eq. (6) one can obtain the value of the universal parameter  $\nu_s$  (see Eq. 4) as

$$\nu_s = -\frac{4}{\tau^2} \ln \left( 1 + \frac{1}{3\tau} \ln(1 - \alpha_v(\tau, \nu_s)) \right). \quad (7)$$

Eqs. (6) and (7) show that experimental values of  $A(\tau, \nu_s)/A(0, \nu_s)$  for any  $\tau$  and  $\rho_c/\rho_g$  determine the universal parameter  $\nu_s = 4\pi R^2 N_s$ . Consequently, the experimental value for  $R$  determines the number of heterogeneous nucleation sites per unit surface,  $N_s = n/(N \cdot S_g)$ .

As mentioned before, this surface crystallization process can be divided in two main steps, each one with a predominant morphological characteristic: (i) 3D-like

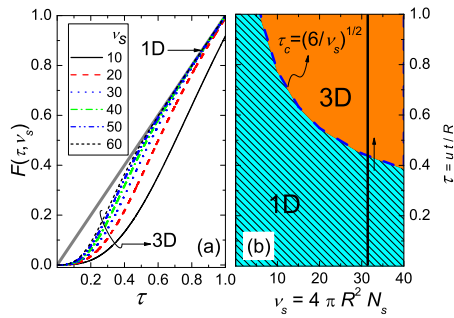


FIG. 3: (a) Function  $F(\tau, \nu_s)$  for various values of  $\nu_s$  (the asymptotic limit  $F(\tau, \nu_s) \rightarrow \tau$  that corresponds to the 1D growth mode is shown). (b) Regions of predominant 1D and 3D modes of crystal growth highlighted in continuous and striped patterns, respectively. Dashed curve: calculated critical parameter  $\tau_c$ , as a function of  $\nu_s$ . Solid vertical line: path corresponding to experimental observations shown in Fig. 1.

crystal growth on the surface and into the volume of glass particles, (ii) when the total surface area of the glass particle is filled with crystals ( $\alpha_s(\tau, \nu_s) \rightarrow 1$ ), the crystal layer continues to grow towards the glass interior in a 1D mode. As this is a continuous transformation of the predominant morphological mode, there is no clear boundary between these two processes. However, our model allows us to characterize this continuous 3D-1D transition in terms of effective parameters and critical values. We can introduce the function  $F(\tau, \nu_s) \equiv \frac{1}{3} \ln(1 - \alpha_v(\tau, \nu_s))^{-1} = \alpha_s(\tau, \nu_s) \cdot \tau$ . The 3D-like crystal growth is “stalled” when  $\alpha_s(\tau, \nu_s) \rightarrow 1$  and this condition corresponds to the asymptotic limit  $F(\tau, \nu_s) \rightarrow \tau$ . In Fig. 3 (a), we show the plots of  $F(\tau, \nu_s)$  for different values of  $\nu_s$ . In order to reach a criterion for the characterization of the transition between the two crystallization modes, we can define a critical dimensionless time,  $\tau_c$ , where  $d^2F(\tau_c)/d\tau^2 = 0$ . This yields an exact value of the critical dimensionless time for the 3D-1D phase transition between the crystallization growth mode given by  $\tau_c = \sqrt{6/\nu_s}$  (depicted in Fig. 3(b)). It is important

to note that this criterion gives, according to Eq. (3), the boundary value for the crystallized surface fraction  $\alpha_s(\tau_c, \nu_s) = 1 - \exp(-\frac{6}{4}) \simeq 0.7769$ , which is independent of  $\nu_s$ . In terms of the critical dimensionless time, Eq. (4) transforms to  $\alpha_s(\tau, \nu_s) = 1 - \exp[-6/4(\tau/\tau_c)^2]$ . A universal phase diagram can be produced, as shown in Fig. 3 (b), which depends only on  $\tau$  and  $\nu_s$  and such a diagram may be used to characterize the crystallization process of spherical glass particles. This is a relevant factor in problems, such as in the control of viscous sintering with concurrent surface crystallization and of the residual porosity in sintered glasses. For instance, one can observe the largest pore highlighted in Fig. 1 (c), which is bound to the crystal formation on the surface of the glass particles. In this case, the experimental DSC values yield a mean value  $\nu_s \sim 31.4$ . According to Eq. (7), this value corresponds to  $N_s \sim 3 \times 10^{11} m^{-2}$  (the approximate experimental path, during the thermal annealing, has been displayed in Fig. 3(b) while the parameters for the diopside glass used in this calculation were:  $u = 2 \cdot 10^{-10} m/s$ ,  $R \sim 5 \mu m$ ,  $\rho_c = 3261 kg/m^3$ ,  $\rho_g = 2805 kg/m^3$ ). The calculated value of the critical dimensionless time for this material yields  $\tau_c = 0.437$ , that corresponds to 3 h of annealing.

In summary, we developed a universal mathematical treatment to deal with the crystallization kinetics of spherical glass particles. Our model has no boundary when passing from the 3D-like crystallization mode on the surface to a 1D-like mode towards the glass interior. We have shown how the area under the DSC crystallization peaks of two samples, one partially crystallized and other glassy, can be used to determine important parameters, such as the number of heterogeneous nucleation sites per unit surface, and the crystallized volume fraction. We have discussed the application limits of this analysis. Finally, we have proposed a phase diagram to characterize the crystallization process of spherical glass particles based on universal parameters.

The authors acknowledge the financial support from the Brazilian agencies FAPESP # 07/08179-9 and CNPq.

\* Now at the DMT, FEG-UNESP, São Paulo, Brazil

- <sup>1</sup> M. L. F. Nascimento, L. A. Souza, E. B. Ferreira, E. D. Zanotto, *J. Non-Cryst. Solids* **351**, 3296 (2005).
- <sup>2</sup> M. O. Prado, E. B. Ferreira, E. D. Zanotto, “Sintering kinetics of crystallizing glass particles. A review.”, Ed. Wiley-Blackwell, *Ceram. Trans.* 170 (2005).
- <sup>3</sup> E. B. Ferreira, M. L. F. Nascimento, H. Stoppa, E. D. Zanotto, *Phys. Chem. Glasses: Eur. J. Glass Sci. Technol. B* **49**, 81 (2008).
- <sup>4</sup> M. L. F. Nascimento, E. B. Ferreira, and E. D. Zanotto, *J. Chem. Phys.* **121**, 8924 (2004).
- <sup>5</sup> R. Müller, *J. Therm. Anal.* **35**, 823 (1989).
- <sup>6</sup> I. Gutzow, R. Pascova, A. Karamanov, and J. Schmelzer, *J. Mater. Sci.* **33**, 5265 (1998).
- <sup>7</sup> J. Vázquez, García-G. Barreda D., P. L. López-Aleman, P. Villares, and R. Jiménez-Garay, *Thermochim. Acta* **430**, 173 (2005).

- <sup>8</sup> A. Kolmogorov, *Izv. Akad. Nauk SSSR, Ser. Matem.* **1**, 355 (1937).
- <sup>9</sup> W. A. Johnson and R. F. Mehl, *Trans. Am. Inst. Min. Metall Eng.* **35**, 416 (1939).
- <sup>10</sup> M. Avrami, *J. Chem. Phys.* **7**, 1103 (1939), *J. Chem. Phys.* **8**, 212 (1940), *J. Chem. Phys.* **9**, 177 (1941).
- <sup>11</sup> J. Farjas, P. Roura, *Phys. Rev. B* **75**, 184112 (2007).
- <sup>12</sup> C. S. Ray, X. Fang, and D. E. Day, *J. Am. Ceram. Soc.* **83**, 865 (2000).
- <sup>13</sup> E. B. Ferreira, L. G. Brunetto, E. D. Zanotto, and V. Lopez-Richard, “DSC determination of the density of surface nucleation sites on glass powders” (to be published).